J Mater Sci: Mater Med (2016) 27:96
DOI 10.1007/s10856-016-5707-4

ENGINEERING AND NANO-ENGINEERING APPROACHES FOR MEDICAL DEVICES

Original Research

Surface morphology, tribological properties and in vitro biocompatibility of nanostructured zirconia thin films

M. Bianchi[1] · A. Gambardella[1] · M. Berni[1] · S. Panseri[2] · M. Montesi[2] · N. Lopomo[3] · A. Tampieri[2] · M. Marcacci[4,5] · A. Russo[1]

Received: 5 February 2016 / Accepted: 14 March 2016 / Published online: 22 March 2016

Abstract Deposition of nanostructured and low-wear zirconia (ZrO_2) thin films on the metallic component of a total joint implant is envisaged to reduce wear of the soft ultra-high molecular weight polyethylene (UHMWPE) counterpart. In this work, morphological surface features, wear resistance and in vitro-biocompatibility of zirconia thin films deposited by the novel Pulsed Plasma Deposition (PPD) method have been investigated. Film thickness, roughness and wettability were found to be strongly dependent on deposition gas pressure. Interestingly, wear rate of UHMWPE disks coupled to zirconia-coated titanium spheres was only poorly correlated to the contact angle values, while film roughness and thickness seemed not to affect it. Furthermore, wear of UHMWPE, when coupled with zirconia coated-titanium spheres, significantly decreased with respect to uncoated spheres under dry or NaCl-lubricated conditions; besides, when using bovine serum, similar results were obtained for coated and uncoated spheres. Finally, suitable mesenchymal stem and osteoblast cells adhesion, proliferation and viability were observed, suggesting good biocompatibility of the nanostructured zirconia films. Taken together, the results shown in this work indicate that zirconia thin films deposited by the PPD method deserve further investigations as low-wear materials for biomedical applications such as total joint replacement.

✉ M. Bianchi
michele.bianchi@ior.it; m.bianchi@biomec.ior.it

[1] Istituto Ortopedico Rizzoli, Laboratorio di NanoBiotecnologie (NaBi), via di Barbiano 1/10, 40136 Bologna, Italy

[2] Institute of Science and Technology for Ceramics, National Research Council of Italy, via Granarolo 64, 48018 Faenza, Italy

[3] Dipartimento di Ingegneria dell'Informazione, Università degli Studi di Brescia, via Branze 38, Brescia, Italy

[4] Istituto Ortopedico Rizzoli, Laboratorio di Biomeccanica e Innovazione Tecnologica, via di Barbiano 1/10, 40136 Bologna, Italy

[5] Dipartimento di Scienze Biomediche e Neuromotorie-DIBINEM, Università di Bologna, via Zamboni 33, 40126 Bologna, Italy

1 Introduction

Titanium (Ti) and its alloys are popular materials in the biomedical field to manufacture orthopedic joints, bone screws and plates, as well as dental and orthodontic implants due to the attractive combination of biocompatibility and mechanical properties (i.e. elastic modulus similar to the one of bone) [1]. However, several concerns have been raised over poor wear resistance of titanium implants and the consequent release of metal ions into body fluids, which has been associated with implant failure [2]. Therefore, research on surface modification or coating of the titanium implants with harder materials able to improve the tribological properties of the metallic surface has been strongly pushed [3, 4]. In particular, several researches have proposed the use of zirconia (zirconium oxide, ZrO_2) in surface modifications due to good chemical stability, corrosion resistance, high wear resistance and higher resistance to brittle fracture than alumina for example [5, 6]. Various coating techniques, including plasma spraying (PS), chemical vapor deposition (CVD), sol–gel method, pulsed laser deposition (PLD) and radio frequency (RF) magnetron sputtering are commonly available for the deposition of zirconia-based coatings and thin films [7–11]. Recently, Pulsed Plasma Deposition (PPD) has been reported to be an innovative and effective method

for the deposition of thin films for photovoltaics, organic electronics and medical applications [12–14]. The possibility to deposit crystalline films even at room temperature, the fidelity over target stoichiometry preservation, the nanostructured texture of the film, the lower scalability costs with respect to comparable techniques such as PLD, are among the most interesting features of PPD technique [15]. We recently proposed the use of a protective zirconia layer deposited by the PPD method in Total Joint Arthroplasty (TJA), with the aim of limiting the wear of the ultra-high molecular weight polyethylene (UHMWPE) insert of the implant. In a series of recent papers, we focused on chemical, micro-structural and nano-mechanical characterization of the zirconia films deposited either on the metallic or plastic components of a TJA implant [16–19]. However, the investigation of the relationship between deposition gas pressure, film surface properties and UHMWPE wear resistance, as well as an in vitro biocompatibility evaluation, are yet to be identified. To bridge this gap, in the present work we firstly characterized the surface properties (i.e. film thickness, roughness and wettability) of zirconia films deposited at different working gas pressure. Subsequently we looked for contingent correlations between surface properties and the tribological behavior of zirconia-coated titanium spheres coupled to UHMWPE disks, thus simulating common mating components in a TJA. Finally, we addressed the proliferation and viability of mouse mesenchymal stem cells and pre-osteoblast cells on zirconia-coated and uncoated titanium substrate.

2 Materials and methods

2.1 Film deposition

Zirconium oxide thin films were fabricated using a Pulsed Plasma Deposition (PPD) system (Gun GEN III, Organic Spintronics S.r.l., Bologna, Italy) by ablating a zirconia target stabilized with 3 mol% yttria (Y_2O_3, ISTEC-CNR, Faenza, Italy). Silicon wafers (*p*-type doped monocrystalline (100) native silicon, size $\sim$20 $\times$ 20 mm, thickness $\sim$3 mm, Fondazione Bruno Kessler, Trento, Italy) were used as substrates for morphological characterizations. Grade 2 titanium spheres (6 mm diameter) and disks (10 mm diameter, 1 mm thickness) were used as substrates for tribological and biological characterizations, respectively. Before deposition, all substrates were ultrasonically cleaned in acetone and isopropanol, then dried under nitrogen flux. The substrates were mounted inside the deposition chamber on a rotating substrate holder positioned at a distance of 65 mm from the surface of the target placed on a rotating target holder. The vacuum chamber was initially evacuated down to a base pressure of 1.0×10^{-7} mbar by a turbomolecular pump (EXT255H, Edwards, Crawley, England) and then raised by controlled flow of oxygen (purity level = 99.999 %) to the following working pressures (mbar): 1.5×10^{-3} (sample henceforth referred to as Zr1.5), 4.0×10^{-3} (Zr4), 6.0×10^{-3} (Zr6), 8.0×10^{-3} (Zr8) and 1.0×10^{-2} (Zr10). Working voltage, current and shot frequency were set at 17.0 kV, 3.0 mA and 5 Hz, respectively. Before each deposition, the target surface was sputter-cleaned for 10.000 shots, keeping the substrate covered by a steel shield. The deposition was performed at room temperature, i.e. without heating the substrate.

2.2 Morphological characterization

Atomic Force Microscopy (AFM) was used to evaluate film thickness, surface roughness and topography. All the measurements were performed with a Stand-alone instrument (NT-MDT, Moscow, Russia) operating in semi-contact mode at ambient conditions. As force sensors for imaging, different Si-cantilevers (NT-MDT, Moscow, Russia) with curvature radius of 10 nm and resonance frequencies of (190–330) kHz were used. The Root Mean Square (RMS) roughness value was chosen as representative of the average surface roughness and it was acquired over different and non-overlapped regions at different scale lengths (scan size from 0.1 to 50 μm). All the images were unfiltered, except for a 2nd order leveling, and acquired with a resolution of 512 $\times$ 512 pixels. The surface wettability of the samples was characterized by contact angle measurement (Digidrop contact angle meter) with distilled water, saline solution (NaCl 0.9 %, Fresenius Kabi Italia S.r.l., Verona, Italy) and fetal bovine serum (75 % v/v deionized water—25 % v/v fetal bovine serum, Cat. N° ECS0180, EuroClone S.p.A, Milan, Italy). Contact angle values were acquired on at least three different positions over the sample's surface and the mean value provided. The volume of the drop was $\sim$50 μl.

2.3 Tribological tests

Tribological tests were carried out using a ball-on-disk tribometer (Anton Paar TriTec SA, Peseux, Switzerland) including a rotating medical grade UHMWPE disk (Citieffe S.r.l., Bologna, Italy) coupled against stationary uncoated and zirconia-coated titanium spheres. The tests were performed applying a normal load of 3 N, for a total of 3000 cycles (cycle length = 3 cm) both under dry and lubricated conditions using a saline solution (NaCl 0.9 %, Fresenius Kabi Italia S.r.l., Verona, Italy) and a solution composed by deionized water (75 % v/v) and fetal bovine serum (25 % v/v, Cat. N° ECS0180, EuroClone S.p.A, Milan, Italy). At the end of the test, on each track at least

five measurements were performed with a contact profilometer (Surtronic 25 Profilometer, Taylor Hobson–Ametek Inc, Berwyn, PA, USA), equipped with a 2 μm round diamond stylus (Small Bore Pick-up 112/1504), in order to calculate the wear volume and consequently the wear rate of the UHMWPE disk, according to Eq. 1:

$$k = V/S * F \quad (1)$$

where k is the wear rate (mm^3/Nm), V is the volume loss (mm^3), S is the sliding distance (m) and F is the load (N).

2.4 In vitro cell cultures

Mouse mesenchymal stem cells (C57BL/6 mMSCs, GIBCO) and mouse pre-osteoblast cell line MC3T3-E1 Subclone 14 (ATCC cell bank) were used for the biological study. In detail, mMSCs were cultured in DMEM Glutamax medium (Gibco) containing 10 % Fetal Bovine Serum (FBS) and 1 % penicillin–streptomycin (100 U/ml-100 μg/mL). MC3T3-E1 were cultured in αMEM containing ribonucleosides, deoxyribonucleosides (GIBCO), 50 μg/ml of ascorbic acid, L-glutamine, 10 % FBS and 1 % penicillin–streptomycin (100 U/ml-100 μg/mL). Both cell cultures were kept at 37 °C in an atmosphere of 5 % CO_2. Cells were detached from culture flasks by tripsinization, centrifuged and resuspended. Cell number and viability were assessed with the trypan-blue dye exclusion test. Each 10 mm-diameter Zr6 and Ti sample was washed in EtOH 70 % for 20 min followed by three washes in PBS 1x for 10 min each. Samples were then air dried and sterilized by UV irradiation for 30 min under laminar flow hood. Samples were placed one per well in a 24-well plate. A drop of 50 μl containing 5.0×10^3 cells (either mMSCs or MC3T3 cells) was seeded on the center of the upper surface of the sample, allowing cell attachment for 40 min in the incubator, before addition into each well of 1 ml of cell culture medium (mMSCs: αMEM Glutamax containing 10 % FBS and 1 % penicillin–streptomycin 100 U/ml-100 μg/mL; MC3T3-E1: αMEM containing ribonucleosides, deoxyribonucleosides, 50 μg/ml of ascorbic acid, L-glutamine, 10 % FBS and 1 % penicillin–streptomycin 100 U/ml-100 μg/mL). The medium was changed every 2 days. All cell-handling procedures were performed in a sterile laminar flow hood. All cell-culture incubation steps were performed at 37 °C with 5 % CO_2.

2.5 Cell proliferation assay

MTT reagent (3-(4,5-dimethylthiazol-2-yl)-2,5-diphenyltetrazolium bromide, Invitrogen) was prepared at 5 mg/ml in 1x PBS. Samples were incubated with the MTT reagent 1:10 for 2 h at 37 °C. Medium was collected and cells incubated with 1 ml of dimethyl sulfoxide for 15 min. In this assay, the metabolically active cells react with the tetrazolium salt in the MTT reagent to produce a formazan dye that can be observed at λ_{max} of 570 nm, using a Multiskan FC Microplate Photometer (Thermo Fisher Scientific Inc) [20]. This absorbance is directly proportional to the number of metabolically active cells. Mean values of absorbance were determined. Three samples per time point (1, 3 and 7 days) were analyzed per group.

2.6 Cell viability assay

Live/Dead assay kit (Invitrogen) was performed according to manufacturer's instructions. Briefly, the samples were washed with 1x PBS for 5 min and incubated with Calceinacetoxymethyl (Calcein AM) 2 μM plus Ethidium homodimer-1 (EthD-1) 4 μM for 15 min at 37 °C in the dark, then they were rinsed in PBS 1x [21]. Images were acquired by an inverted Nikon Eclipse Ti-E fluorescence microscope (Nikon, Tokyo, Japan). One sample per group was analyzed at day 1 and day 3.

2.7 Cell morphology evaluation

One sample per group was used for actin detection by Scanning Electron Microscope (SEM) and fluorescence analysis respectively at day 1 and day 3 of cell culture. In order to visualize actin filaments samples were washed with PBS 1x for 5 min, fixed with 4 % (w/v) paraformaldehyde for 15 min and washed with PBS 1x for 5 min. Permeabilization was performed with PBS 1x with 0.1 % (v/v) Triton X-100 for 5 min. FITC-conjugated Phalloidin antibody (Invitrogen) 38 nM in PBS 1x was added for 20 min at room temperature in the dark [22]. Cells were washed with PBS 1x for 5 min and incubated with nuclear stain DAPI (Invitrogen) 300 nM in PBS 1x for 5 min. The nuclear morphological changes were also evaluated. Images were acquired by an inverted Nikon Eclipse Ti-E fluorescence microscope (Nikon, Tokyo, Japan). For SEM analysis, after 1 day of cell culture, one sample per group was washed with 0.1 M sodium cacodylate buffer pH 7.4 and fixed in 2.5 % glutaraldehyde in 0.1 M sodium cacodylate buffer pH 7.4 for 2 h at 4 °C, washed in 0.1 M sodium cacodylate buffer pH 7.4 and dehydrated in a graded series of ethanol for 10 min each. Dehydrated samples were sputter-coated with gold and observed using a Quanta Scanning Electron Microscope (ESEM Quanta 200, Fei).

2.8 Statistical analysis

Results of the tribological tests were expressed as mean ± SD and statistically analyzed using one-way ANOVA with the Tukey HSD post hoc test to detect

differences among groups, with statistical significance set at $P \leq 0.05$. Results of the biological tests were expressed as mean ± SEM plotted on graph. Analysis was made by two-way ANOVA, followed by Bonferroni's post hoc test. Statistical analysis was performed by the GraphPad Prism software (version 5.0), with statistical significance set at $P \leq 0.05$.

3 Results

3.1 Morphological analysis

Average thickness, roughness and wettability of zirconia thin films deposited by the PPD method using different gas pressures during deposition are reported in Table 1.

Results shown in Table 1 indicate that gas pressure inside the deposition chamber has a strong influence on the morphological features of the deposited films. In particular, film thickness is dramatically influenced, ranging from values as small as 50 nm at 1.5×10^{-3} mbar up to 800 nm at 8.0×10^{-3} mbar. By further increasing gas pressure, film thickness starts to decrease. Surface roughness and contact angle follow a very similar trend (see also Fig. 1g), maximum values being obtained for intermediate values of gas pressure. Interestingly, contact angle values covers a rather wide range of water affinity, switching from a wetting regime (50° ÷ 60°) at higher and lower pressure values, to a poorly-wetting regime (80° ÷ 90°) for intermediate pressure values.

AFM analysis at the sub-micron scale (Fig. 1) points out that film surface mainly consists of round-shaped grains with average size ranging from few tens of nanometers to about 200 nm, exhibiting increasing packing density along with gas pressure increase (Fig. 1a–e). Analysis of AFM images acquired at lower magnification indicates a homogenous morphology with no surface defects for areas as large as (50×50) μm^2 (data not shown). It can be also observed that surface roughness saturates at scan areas larger than about (20×20) μm^2 for the entire dataset (Fig. 1f): this circumstance allows to consider the averaged RMS values obtained at the maximum scan area as representative of each sample, so that the evolution of roughness with pressure can be followed together with the corresponding contact angles values, as shown in Fig. 1g.

3.1.1 Tribological tests

Wear rate of UHMWPE disks after 3000 cycles is significantly lower when the plastic disk is coupled with zirconia-coated titanium spheres (independently from deposition pressure), compared to uncoated titanium, both under dry and NaCl-lubricated conditions (Table 2). When using bovine serum as lubricant, wear values are comparable to the ones using uncoated titanium spheres.

UHMWPE wear rate values, obtained under dry and lubricated conditions, have been plotted against zirconia film thickness (Fig. 2a), RMS (Fig. 2b) and contact angle (Fig. 2c) in order to highlight contingent correlations between wear and film features. Only very weak correlations have been found among wear rate and contact angle values ($R^2 = 0.6843$ in serum, $R^2 = 0.6658$ in saline solution), with lower (50° ÷ 60°) and higher (80° ÷ 90°) contact angles values leading to lower wear of the UHMWPE compared to intermediate values. No correlation with $R^2 > 0.6$ has been found in all the other investigated cases. Interestingly, sample Zr6, exhibiting the highest RMS and contact angle values, shows the lowest wear among the coated samples. Finally, Fig. 2 also puts into evidence a higher scattering of data collected under dry conditions compared to those obtained under lubricated conditions, suggesting that the latter tend to mitigate the effect of surface features of the films compared to dry conditions.

The surface of coated and uncoated titanium spheres has been investigated by optical microscopy at the end of the test in order to evaluate film abrasion/detaching (Fig. 3). A severe coating delamination and ploughing-like scratches are detected for films deposited at lower (Zr1.5, Fig. 3a–c) and higher (Zr10, Fig. 3g–I) pressure, especially under lubricated conditions. On the contrary, the surface of Zr6 results free of evident wear phenomena under all the three different conditions (Fig. 3d–f), similarly to what observed for uncoated titanium relatively to dry (Fig. 3j) and NaCl-

Table 1 Summary of thickness, surface roughness and contact angle data of zirconia thin films deposited by the PPD method operating at oxygen pressure ranging from 1.5×10^{-3} to 1.0×10^{-2} mbar. RMS values are calculated on a 50×50 μm^2 scanned area

Film	Zr1.5	Zr4	Zr6	Zr8	Zr10
Working gas pressure (mbar)	1.5×10^{-3}	4.0×10^{-3}	6.0×10^{-3}	8.0×10^{-3}	1.0×10^{-2}
Thickness (nm)	50 ± 10	200 ± 10	600 ± 50	800 ± 100	550 ± 100
RMS (nm)	24 ± 2	32 ± 2	40 ± 1	37 ± 1	35 ± 1
CA_{NaCl} (°)	55 ± 3	82 ± 4	88 ± 4	76 ± 5	63 ± 3
CA_{Serum} (°)	56 ± 3	86 ± 4	87 ± 4	77 ± 5	62 ± 2

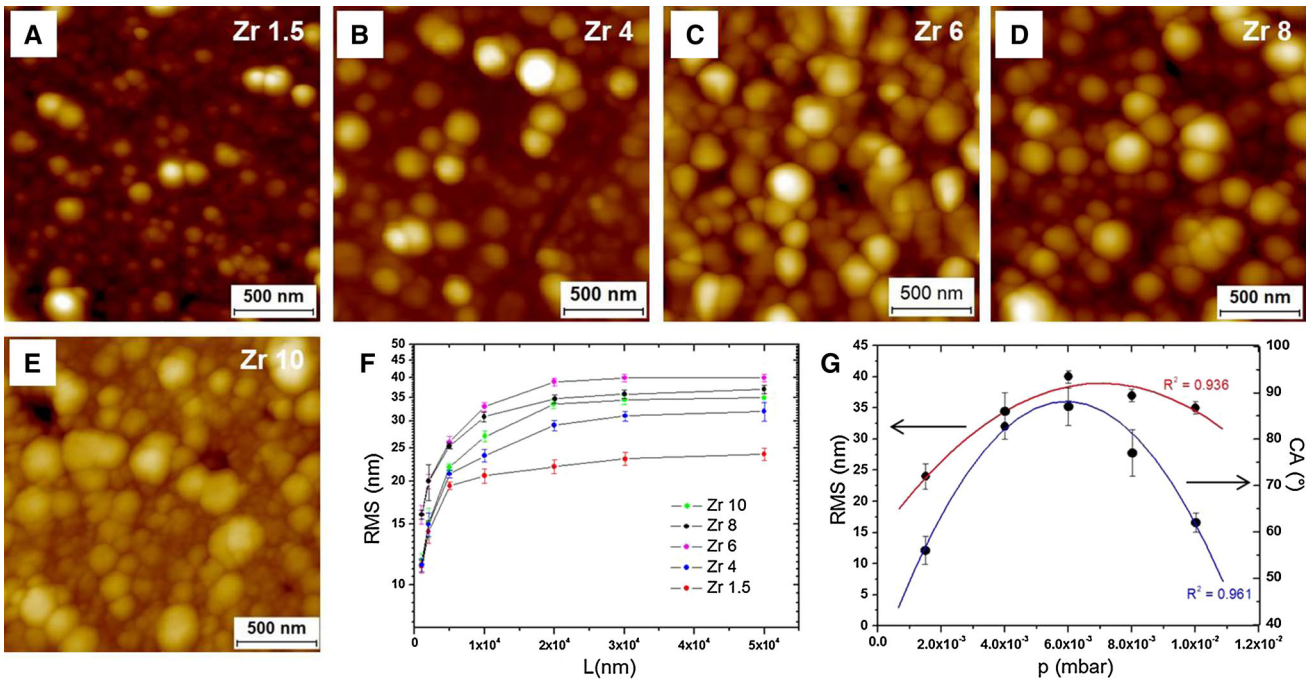

Fig. 1 **a–e** Representative AFM topographical images (2 × 2 μm^2) of zirconia films deposited at oxygen pressure values ranging from 1.5 × 10^{-3} to 1 × 10^{-2} mbar; **f** plot of the log(RMS) versus lateral image size; **g** trend of RMS roughness and contact angle in serum versus working gas pressure

Table 2 Wear rate of UHMWPE polyethylene disks coupled with coated (Zr1.5, Zr4, Zr6, Zr8 and Zr10) and uncoated titanium balls after 3000 cycles under dry and lubricated conditions

	Water rate	(×10^{-4} mm^3/Nm)	
	Dry	NaCl	Serum
Zr1.5	7.2 ± 0.5*	4.8 ± 0.3*	4.9 ± 0.4
Zr4	5.7 ± 0.5*	5.0 ± 0.5*	5.0 ± 0.2
Zr6	6.3 ± 0.5*	4.8 ± 0.3*	4.5 ± 0.4§
Zr8	6.3 ± 0.7*	5.0 ± 0.2*	5.4 ± 0.2
Zr10	7.3 ± 0.8*	4.8 ± 0.3*	5.0 ± 0.3
Uncoated titanium	10.2 ± 0.5*	5.7 ± 0.3	5.0 ± 0.2

* Refers to $P < 0.05$ versus uncoated titanium; § refers to $P < 0.05$ versus Zr8

lubricated (Fig. 3k) conditions. Noteworthy, when using serum, evident abrasion scratches occur on the surface of bare titanium (Fig. 3l), whereas the presence of a thin layer of zirconia seems to protect the underlying metal from strong wear.

3.1.2 In vitro cell analysis

In view of their superior tribological properties with respect to the other films, biological evaluation of mMSCs and pre-osteoblasts MC3T3-E1 proliferation, viability and morphology has been performed on Zr6 films and on bare Ti samples as control. In detail, quantification of metabolically active cells has been performed for each time point. MTT test results demonstrate an increase in cell proliferation from day 1 to day 7 for all the samples with both cell types, highlighting the absence of cytotoxicity of the zirconia layer (Fig. 4a, b). The only statistically significant difference among the groups has been identified for mMSCs at day 7. Noteworthy, Zr6 sample shows a slight increase in cell proliferation compared to the control Ti group (Fig. 4a).

The cell cultures have been also analyzed for cell viability with the Live/Dead assay based on the simultaneous determination of live and dead cells with two probes, Calcein and EthD-1, that measure recognized parameters of cell viability: i.e. intracellular esterase activity and plasma membrane integrity, respectively. A very high ratio of viable cells is observed, with no significant differences between Zr6 and Ti group for both cell types (Fig. 4c–f). Moreover, the nuclear morphological qualitative analysis confirms that Zr6 samples are not cytotoxic. In fact, the nuclei of MSCs and MC3T3 cells seeded on the samples show their native morphology and none abnormal alterations have been detected (e.g. nuclear fragmentation, chromatin condensation) (Fig. 4g–l).

In addition, cell morphology has been analyzed by phalloidin staining and scanning electron microscopy. In

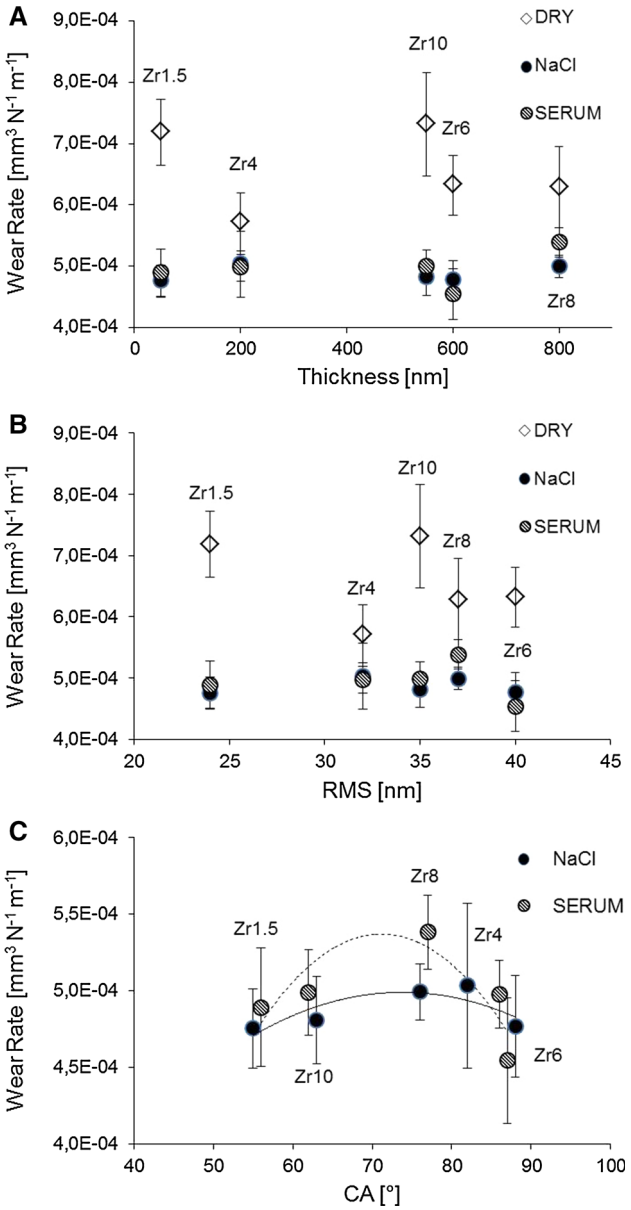

Fig. 2 UHMWPE wear rate as a function of zirconia film thickness (**a**), RMS (**b**) and contact angle (**c**), obtained under dry, saline and serum lubricated conditions. In **c**, *continuous line* represents the trend line for data obtained in saline solution, whereas *dotted line* represents the trend line for data obtained in serum

particular, organization of the cytoskeletal structure of actin filaments is an essential element in maintaining and modulating cellular morphology and cell structural integrity. The morphological analysis shows that MSCs and MC3T3-E1 cells well adhere to Zr6 samples without any difference compared to Ti control group (Fig. 5a, b, d, e). In detail, MSCs and MC3T3-E1 show their typical spindle/fibroblast-like morphology and polygonal shape, respectively (Fig. 5a, b, d, e). Moreover, a detailed cell morphology SEM analysis performed at 24 h from seeding, indicate cells are firmly attached to the samples surface, without any differences among the groups (Fig. 5c, f).

4 Discussions

In the present manuscript we investigated the possibility to reduce wear of the plastic insert of a joint implant by the addition of a nanostructured zirconia layer on the metallic counterpart, deposited by the PPD system. We started by showing the influence of the working gas pressure on the morphological parameters of zirconia thin films. The significant influence of gas pressure on the final morphological surface features and on thickness in particular, can be explained recalling the fact that within the PPD process, gas pressure influences all the main operative steps, i.e. plasma initiation, evolution and propagation [23]. Briefly, PPD method is based on a fast (200–400 nsec) pulsed (5–100 Hz) flow of high-energy electrons impinging on a target material, transferring its energy to the target material through a non-equilibrium temperature distribution process and eventually causing its ejection (ablation process) [23]. Immediately after ablation, the ablated material (so called "plasma plume") is deposited on a substrate held at suitable distance. Thus, the ablation capacity is directly related to the intensity of the electron flow. In turn, the flow of electrons is generated with the extraction of electrons from an initial plasma, created on walls of a metallic hollow cathode, which are then accelerated by the application of a potential difference (up to 20 kV) between the cathode and target material (anode). The amount of initiating plasma strictly depends on the amount of gas available in the chamber. Thus, at lower pressure, a low number of electrons is extracted from the plasma and accelerated to the target, causing poor ablation of the target. It follows that the final thickness of the films is very low [24]. By increasing gas pressure, and thus the density of the initiating plasma, more electrons are extracted and accelerated and a more effective ablation process occurs leading to thicker films. However, at very high pressure values (i.e. above 1×10^{-2} mbar), the energy of the plasma strongly decreases due to the occurring of beam energy dissipation phenomena, such as extended plasma generation, partial heating and other processes [25]. Furthermore, at high pressure values, also an increased number of collisions between plasma plume material and gas molecules within the deposition chamber contributes to lower the deposition rate and thus the thickness of the growing film.

Surface roughness and wettability of an implant material are among the most important parameters influencing protein adsorption dynamics and thus cell adhesion and proliferation [26, 27]. As observed, the trends of surface

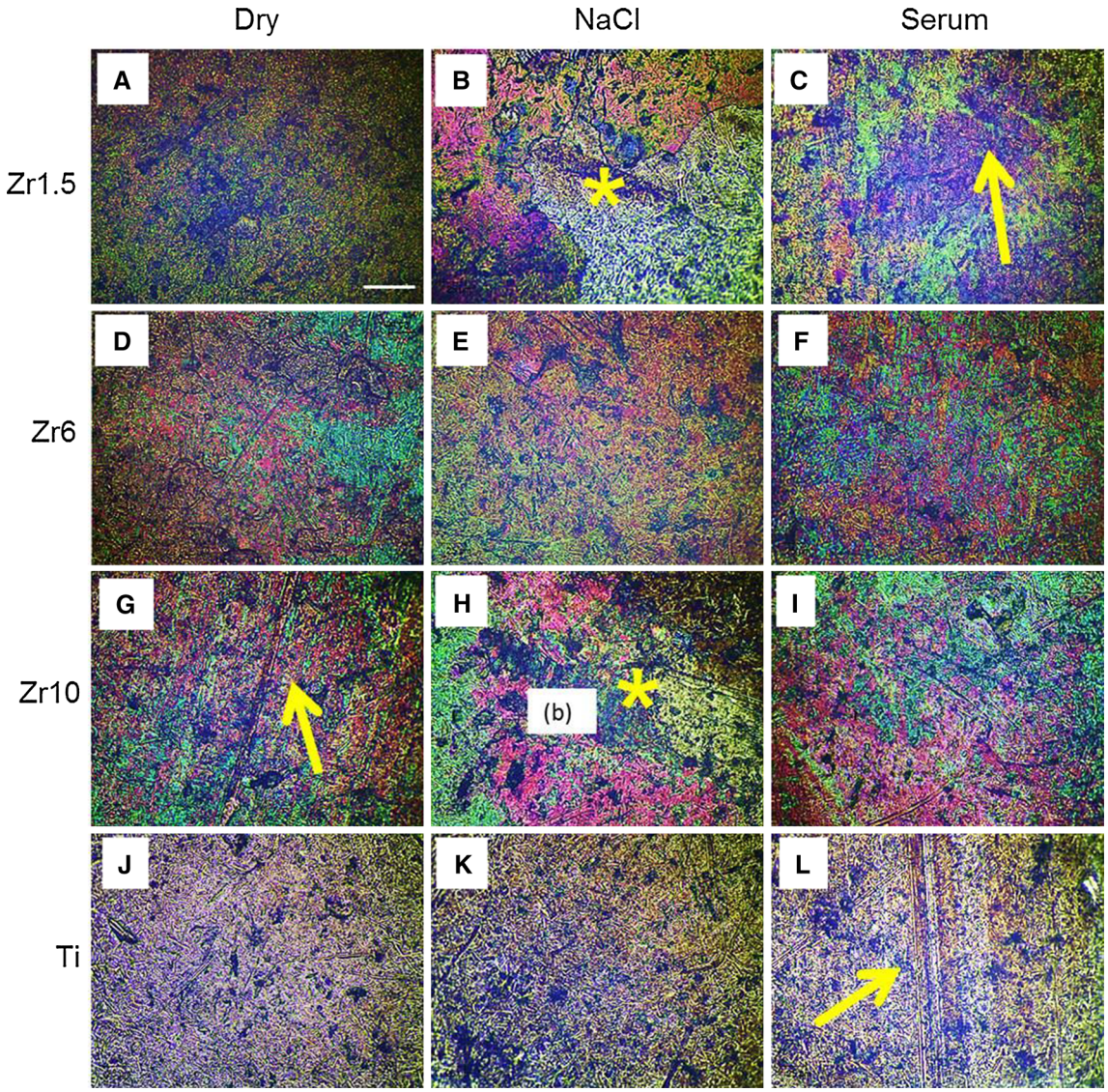

Fig. 3 Optical images of the worn surface of Zr1.5 (**a**–**c**), Zr6 (**d**–**f**), Zr10 (**g**–**i**)-coated and uncoated (**j**–**l**) titanium spheres after the tribological tests under dry (**a**, **d**, **g**, **j**), saline solution (**b**, **e**, **h**, **k**) and bovine serum lubricant (**c**, **f**, **i**, **l**). *Yellow stars* mark the worn region of the coated spheres where the coating detached. *Yellow arrows* indicate the worn area where ploughing wear mode occurred. Scale bar (in A) is 50 μm for all the panels

roughness and contact angle are strictly related to that of thickness. The higher the film thickness, the higher the surface roughness, as a consequence of the occurrence of aggregation and coalescence phenomena the make the film surface growth more disordered when compared to the smooth and homogenous first layers, as well known for PVD processes [28]. The dependence of contact angle value and hence of surface wettability upon surface roughness found in the present work fits well with literature investigating the impact of roughness on the wettability of a solid substrate. In detail, it has been widely reported that surface roughness is able to enhance the intrinsic non-wetting chemistry of the surface, to such an extent that even super non-wetting surfaces can be produced [29]. There is general agreement also on the fact that a low contact angle value, i.e. high surface energy, is able to promote greater cell adhesion when compared to high contact angle value, i.e. low surface energy [30]. Zirconia films deposited by the PPD method span a wide spectrum of contact angles values, ranging from $\sim 50°$ to $\sim 90°$, hence being suitable for cell growth and viability. Among all the investigated surface features, wettability is shown to be the characteristic that best correlates with tribological results. Notably and interestingly for industrial application,

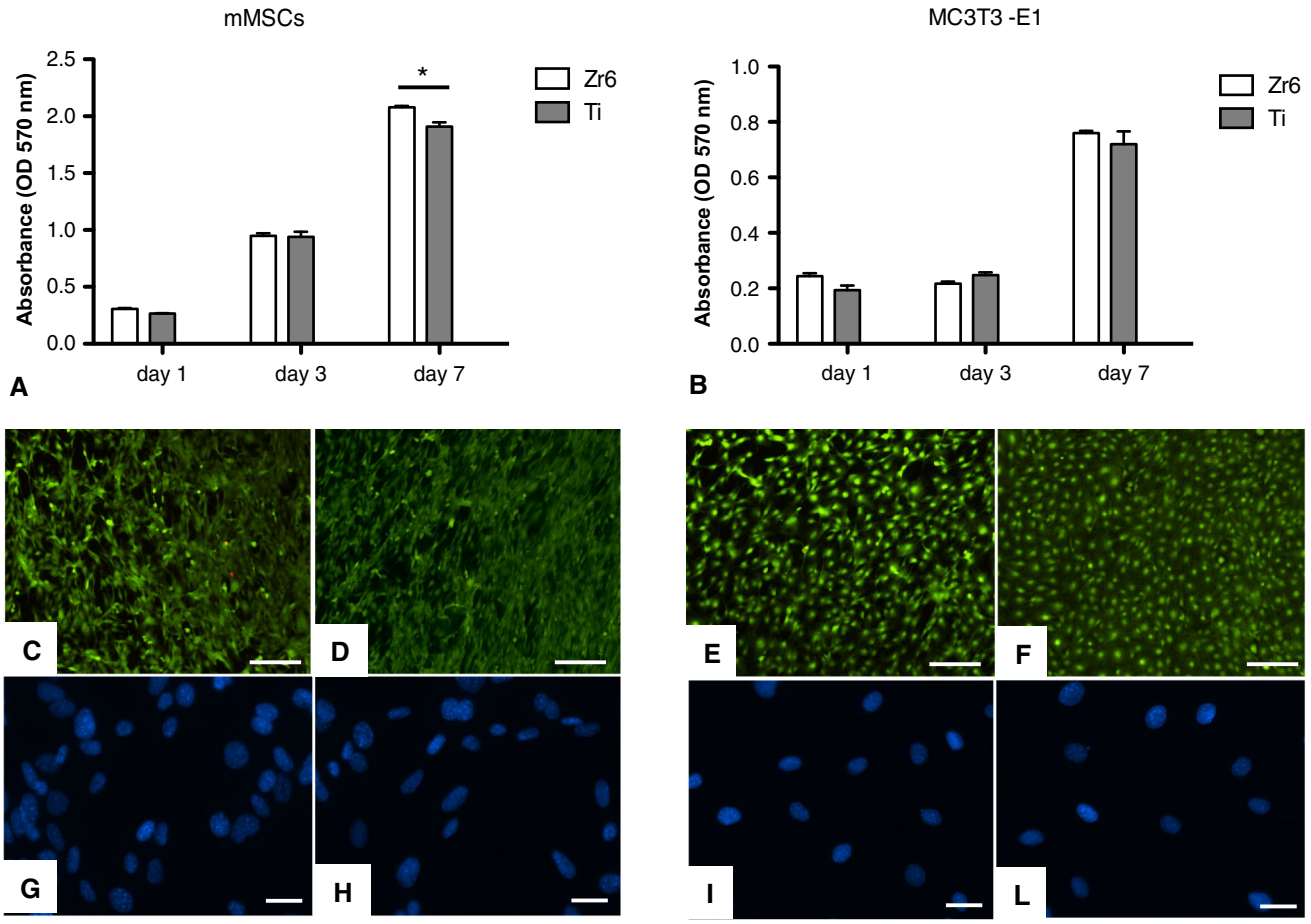

Fig. 4 Analysis of cells proliferation by MTT assay, after 1, 3 and 7 days of MSCs (**a**) and MC3T3-E1 (**b**) cells seeded on the samples. $*p \leq 0.01$; $n = 3$. Cell viability was analyzed by the live/dead assay. Calcein AM stains for live cells in green, EthD-1 stains for dead cells in red. **c** and **d** showed MSCs, and **e** and **f** showed MC3T3-E1 seeded on Zr6 and Ti samples respectively after 3 days. Nuclear morphological analysis showed physiological nuclear shape of MSCs and MC3T3-E1 cells seeded on Zr6 and Ti samples, respectively, after 1 day. *Scale bars* are 200 μm in C-F and 25 μm in **g–l** (Color figure online)

by acting on gas pressure it is possible to properly select film surface features and thus to obtain UHMWPE wear rate values similar (in serum solution) or better (in saline solution or dry conditions), compared to the bare titanium substrates. In this perspective, it can be noted that the best performing zirconia thin film, in terms of wear rate, is Zr6, that is the sample showing the highest roughness and, consequently, the highest contact angle. Concerning lubrication, contrary to what expected, the worse tribological behavior exhibited by the coated samples in serum solution is probably due to the occurrence of the previously highlighted partial delamination of the thin film. Several imperfections, generated during the deposition process, may represent proper initiation sites for wear phenomena—such as pitting and stress-induced cracks—and corrosion, both encouraged by the presence of biological species in solution, and hence result in a delamination process [31]. These effects were predominant compared to the proper lubrication action exerted by the serum, which was also influenced by the thin film wettability compared to bare titanium samples. Furthermore, the cracks advancement promotes serum penetration through the thin film and the formation of blisters, which are the basis of the occurrence of local delamination phenomena [31]. Zirconia is a well-known biocompatible material already extensively used in medicine and TJA in particular; [5] however, the cytotoxicity of nanostructured zirconia films deposited by PPD method has not been addressed yet. Thus, preliminary in vitro biological evaluation has been carried out by investigating adhesion, proliferation, viability and morphology of mesenchymal stem cells and pre-osteoblasts cell lines. Noteworthy, the results of the biological tests highlighted the absence of cytotoxicity due to the nanostructured texture of the surface and an overall good biocompatibility of the films when compared to uncoated titanium, used as control.

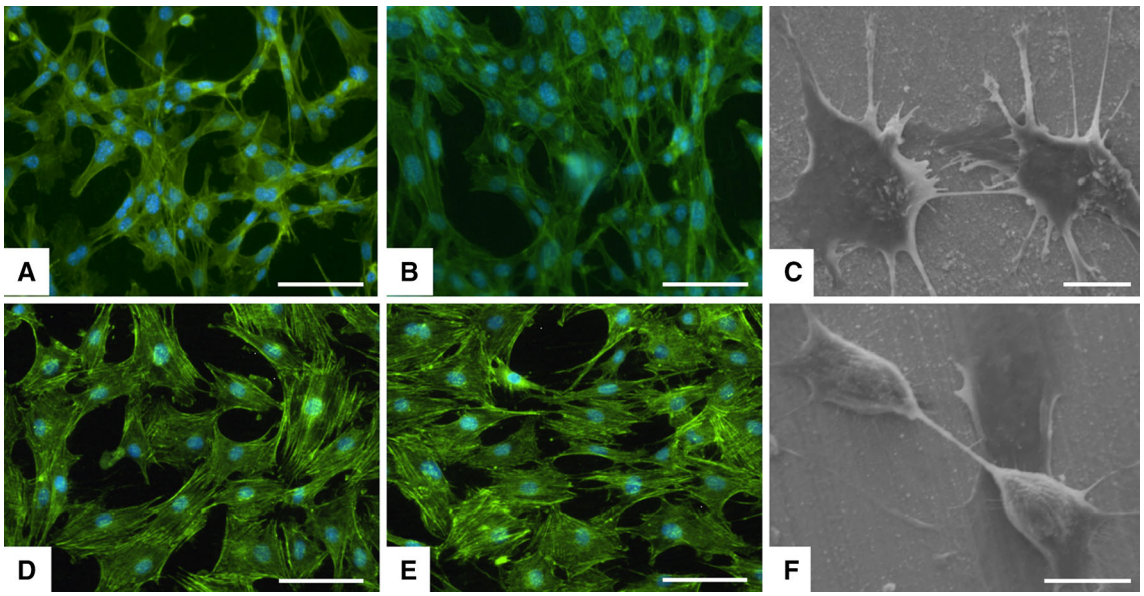

Fig. 5 Analysis of cell morphology by phalloidin staining (**a**, **b**, **d**, **e**). MSCs were spread with good morphology and firmly attached to the Zr6 (**a**) and Ti (**b**) samples after 3 days. Similar results were detected with MC3T3-E1 cells on Zr6 (**d**) and Ti (**e**) samples after 3 days. Phalloidin in green stains for actin filaments and DAPI in blue stains for cell nuclei. SEM analysis of attached MSCs (**c**) and MC3T3-E1 (**f**) cell morphology after 24 h on the surface of Zr6 samples respectively. *Scale bars* are 100 μm in panels **a**, **b**, **d**, and **e**; 10 μm in panels **c** and **f**

5 Conclusions

Nanostructured zirconia films deposited on titanium by the PPD method cause reduced wear of the UHMWPE counterpart after 3000 cycles under dry or NaCl-lubricated conditions when compared to bare titanium, whereas a reduction of these beneficial effects is experienced in serum-fluid, regardless deposition conditions. The different behavior of the film in NaCl compared to serum could be attributed to a greater corrosive effect of the biological species that are present in the latter. Consequently, a preliminary detrimental effect of the serum-lubricant on the tribological performance of the fabricated ceramic film was highlighted in this study. This issue presented a multifactorial cause: the coating was in fact affected by both the presence of the fluid itself and by the high values of contact pressure considered during the testing, which indeed represented one of the most severe conditions. However, even considering different applications in orthopedic, the biocompatibility and the preliminary tribological tests suggest to continue pursuing the study of these ceramic films realized by PPD, possibly introducing manufacturing improvements such as tailoring their nanostructure by using a more hydrophilic compound as target material or investigating the possibility of heating the coating after the deposition, thus reducing crack formation and fluid penetration and enhancing adhesion and resistance to lubricant effect. Further tests will be required to clarify the wear process of zirconia-coated titanium under both dry and wet conditions.

Acknowledgments The study was supported by the project "Nanostructured Coatings Enhancing Material Performances in Joint Arthroplasty" (project code: GR-2010-2312686), funded by the Italian Ministry of Health and co-funded by the Istituto Ortopedico Rizzoli. The authors would like to particularly thank Carmelo Carcasio for his support in mechanical manufacturing, Dr. Simone Sprio (Institute of Science and Technology for Ceramics, National Research Council of Italy) and Dr. Maria Cristina Maltarello (Laboratorio di Biologia Cellulare Muscoloscheletrica, Istituto Ortopedico Rizzoli) for providing the zirconia targets and the lubricants for the tribological tests, respectively.

References

1. Dalmiglio M, Schaaff P, Holzwarth U, Chiesa R, Rondelli G. The effect of surface treatments on the fretting behavior of Ti–6Al–4 V alloy. J Biomed Mater Res A. 2008;86B:407–16.
2. Dong H, Shi W, Bell T. Potential of improving tribological performance of UHMWPE by engineering the Ti6Al4 V counterfaces. Wear. 1999;225–229:146–53.
3. Rautray TR, Narayanan R, Kim K. Ion implantation of titanium based biomaterials. Prog Mater Sci. 2011;56:1137–77.
4. Wu H, Zhang X, He X, Li M, Huang XB, Hang RQ, Tang B. Wear and corrosion resistance of anti-bacterial Ti–Cu–N coatings on titanium implants. Appl Surf Sci. 2014;316:614–21.
5. Piconi C, Maccauro G. Zirconia as a ceramic biomaterial. Biomaterials. 1999;20:1–25.
6. Kaluđerović MR, Schreckenbach JP, Hans-Ludwig Graf H. Zirconia coated titanium for implants and their interactions with osteoblast cells. Mater Sci Eng C 2014;44:254–61.

7. Dong H, Yang G, Cai H, Ding H, Li C, Li C. The influence of temperature gradient across ZIRCONIA on thermal cyclic lifetime of plasma-sprayed thermal barrier coatings. Ceram Int. 2015;41:11046–56.
8. Torres-Huerta AM, Dominguez-Crespo MA, Onofre-Bustamante E, Flores-Vela A. Characterization of ZrO_2 thin films deposited by MOCVD as ceramic coatings. J Mater Sci. 2012;47:2300–9.
9. Catauro M, Bollino F, Papale F. Biocompatibility improvement of titanium implants by coating with hybrid materials synthesized by sol–gel technique. J Biomed Mater Res A. 2014;102:4473–9.
10. Hidalgo H, Reguzina E, Millon E, Thomann AL, Mathias J, Boulmer-Leborgne C, Sauvage T, Brault P. Yttria-stabilized zirconia thin films deposited by pulsed-laser deposition and magnetron sputtering. Surf Coat Technol. 2011;205:4495–9.
11. Sprio S, Guicciardi S, Bellosi A, Pezzotti G. Yttria-stabilized zirconia films grown by radiofrequency magnetron sputtering: Structure, properties and residual stresses. Surf Coat Technol. 2006;200:4579–85.
12. Huang YW, Li GF, Feng JH, Zhang Q. Investigation on structural, electrical and optical properties of tungsten-doped tin oxide thin films. Thin Solid Films. 2010;518:1892–6.
13. Dediu V, Hueso LE, Bergenti I, Riminucci A, Borgatti F, Graziosi P, Newby C, Casoli F, De Jong MP, Taliani C, Zhan Y. Room-temperature spintronic effects in Alq3-based hybrid devices. Phys Rev B. 2008;78:115203.
14. Boi M, Bianchi M, Gambardella A, Liscio F, Kaciulis S, Visani A, Barbalinardo M, Valle F, Iafisco M, Lungaro L, Milita S, Cavallini M, Marcacci M, Russo A. Tough and adhesive nanostructured calcium phosphate thin films deposited by the pulsed plasma deposition method. Rsc Adv. 2015;5:78561–71.
15. Bianchi M, Russo A, Taliani C, Marcacci M. Pulsed plasma deposition (PPD) technique, dekker encyclopedia of nanoscience and nanotechnology, 3rd edn. CRC Press; 2015. doi:10.1081/E-Enn3-120053233.
16. Bianchi M, Russo A, Lopomo N, Boi M, Maltarello MC, Sprio S, Baracchi M, Marcacci M. Pulsed plasma deposition of zirconia thin films on UHMWPE: proof of concept of a novel approach for joint prosthetic implants. J Mater Chem B. 2013;1:310–8.
17. Bianchi M, Boi M, Lopomo N, Maltarello MC, Liscio F, Milita S, Visani A, Russo A, Marcacci M. Nanomechanical characterization of zirconia thin films deposited on UHMWPE by pulsed plasma deposition. J Mech Med Biol. 2015;15:1550070.
18. Bianchi M, Lopomo N, Boi M, Gambardella A, Marchiori G, Berni M, Pavan P, Marcacci M, Russo A. Ceramic thin films realized by means of pulsed plasma deposition technique: applications for orthopaedics. J Mech Med Biol. 2015;15:1540002.
19. Marchiori G, Lopomo N, Boi M, Berni M, Bianchi M, Gambardella A, Visani A, Russo A, Marcacci M. Optimizing thickness of ceramic coatings on plastic components for orthopaedic applications: a finite element analysis. Mat Sci Eng C. 2016;58:381–8.
20. Liu Y, Peterson DA, Kimura H, Schubert D. Mechanism of cellular 3-(4,5-dimethylthiazol-2-yl)-2,5-diphenyltetrazolium bromide (MTT) reduction. J Neurochem. 1997;69:581–93.
21. Papadopoulos NG, Dedoussis GV, Spanakos G, Gritzapis AD, Baxevanis CN, Papamichail M. An improved fluorescence assay for the determination of lymphocyte-mediated cytotoxicity using flow cytometry. J Immunol Methods. 1994;177:101–11.
22. Faulstich H, Zobeley S, Rinnerthaler G, Small JV. Fluorescent phallotoxins as probes for filamentous actin. J Muscle Res Cell Motil. 1988;5:370–83.
23. Yarmolich D, Nozar P, Gleizer S, Krasik YE, Mittica G, Ancora C, Brillante A, Bilotti I, Taliani C. Characterization of deposited films and the electron beam generated in the pulsed plasma deposition gun. Jpn J Appl Phys. 2011;50:08JD03.
24. Gleizer S, Yarmolich D, Felsteiner J, Krasik YE, Nozar P, Taliani C. Electron beam and plasma modes of a channel spark discharge operation. J Appl Phys. 2009;106:073301.
25. Graziosi P, Prezioso M, Gambardella A, Kitts C, Rakshit RK, Riminucci A, Bergenti I, Borgatti F, Pernechele C, Solzic M, Pullini D, Busquets-Mataixa D, Dediu VA. Conditions for the growth of smooth $La_{0.7}Sr_{0.3}MnO_3$ thin films by pulsed electron ablation. Thin Solid Films. 2013;534:83–9.
26. Wei J, Igarashi T, Okumori N, Igarashi T, Maetani T, Liu B, Yoshinari M. Influence of surface wettability on competitive protein adsorption and initial attachment of osteoblasts. Biomed Mater. 2009;4:045002.
27. Bianchi M, Urquia Edreira ER, Wolke JGC, Birganic ZT, Habibovic P, Jansen JA, Tampieri A, Marcacci M, Leeuwenburgh SCG, van den Beucken JJJP. Substrate geometry directs the in vitro mineralization of calcium phosphate ceramics. Acta Biomater 2014;10:661–9.
28. Petrov I, Barna PB, Hultman L, Greene JE. Microstructural evolution during film growth. J Vac Sci Technol, A. 2003;21:S117.
29. Herminghaus S. Roughness-induced non-wetting. Europhys Lett. 2000;52:165.
30. Att W, Takeuchi M, Suzuki T, Kubo K, Anpo M, Ogawa T. Enhanced osteoblast function on ultraviolet light-treated zirconia. Biomaterials. 2009;30:1273.
31. Escudeiro A, Wimmer MA, Polcar T, Cavaleiro A. Tribological behavior of uncoated and DLC-coated CoCr and Ti-alloys in contact with UHMWPE and PEEK counterbodies. Tribol Int. 2015;89:97–104.